Tensile Deformation Behavior of Carbon Nanotube Junctions

W.C. Liu[1], F.Y. Meng[2] and S.Q. Shi*[1]

[1]Department of Mechanical Engineering, The Hong Kong Polytechnic University, Hong Kong, China
[2]Department of Applied Physics, University of Science and Technology Beijing, Beijing, China
*Corresponding author: Tel: +852 2766 7821, Fax: +852 2365 4703, E-mail: mmsqshi@polyu.edu.hk

ABSTRACT

Deformation behavior of five types of X-junctions made from ultrathin single-walled carbon nanotubes has been investigated using molecular dynamics (MD) simulation. Three different deformation modes were observed. If the junction is strong, such as some (3,3)-(3,3) junctions, bonds will be broken at individual nanotubes rather than at the junction region. In this case, original bonding structures around the X-junctions will be maintained. However, for some other (3,3)-(3,3) junctions and those X-junctions formed by (5,0)-(5,0) nanotubes, bonds at the junction region were broken and reconstructed under tensile load. This resulted in the transformation of 3-D junctions into a 2-D type. Either one neck or two necks may be nucleated near the junction. Random seed numbers used in MD simulations plays an important role in the outcomes of the deformation process, which is due to the small number of carbon atoms involved in the junction regions.

Keywords: single-walled carbon nanotubes, X-junctions, molecular dynamics simulation, mechanical properties

1 INTRODUCTION

Since the discovery of carbon nanotubes (CNTs) in 1991 [1], the properties of CNTs have been widely studied experimentally and theoretically. It was found that CNTs have superior mechanical, physical, electrical and chemical properties [2-4]. For example, Young's modulus of single-walled CNTs reported in the literature is mostly between 0.9TPa ~ 1.2TPa [5,6], which attracted many studies on the factors that affect mechanical properties of CNTs reinforced nanocomposites [7,8]. CNTs also possess chirality-dependent electrical conductivity. Some believe that CNTs may break the size limit of current silicon-based technology and become the building blocks for the next-generation of electronic devices. One of such building blocks may be single-walled carbon nanotube (SWCNT) junctions [9]. Three-terminal SWCNT junctions (T or Y-junctions) or four-terminal SWCNT junctions (X junctions) are most interesting because the third or fourth terminal may be used to control the power gain and/or switching mechanism. Then, electronic properties and mechanical properties of its junctions are being studied. Cleri reported a tight binding MD study of electronic properties of junctions between (5,5) SWCNTs with an increasing degree of disorder in the connected region [10]. Jang investigated covalent junctions formed between various types of crossed SWCNTs under electron beam irradiation and the mechanical responses of (5,5)-(5,5) junctions under stresses [11]. The mechanical properties of intramolecular junctions (IMJs) formed by connecting the ends of two SWCNTs with different diameters are being studied recently [12-15]. The junctions studied above are all two dimensional (2-D) junctions, i.e., the connection or two crossing CNTs and the junction region are laying in the same plane.

Our group had simulated the welding process of two crossed ultrathin carbon nanotubes without pre-existing structural defects by the direct heating method [16]. Most of the junctions formed this way are 3-D junctions, i.e., the two crossing tubes are not in the same plane. Five possible structures of these 3-D junctions can be found. Meng et al. has roughly investigated the mechanical properties of these 5 types of junctions under uni-axial tension [17]. In this work, we investigate the mechanical properties of these X-junctions under uni-axial and bi-axial stresses systematically.

2 METHODOLOGY AND GEOMETRY OF JUNCTIONS

Using second-generation reactive empirical bond order (REBO) potential [18] as the input for our molecular dynamic simulation program, mechanical properties of 3-D X-junctions under stresses were investigated. We consider X-junctions formed by two single-walled nanotubes with (3,3) x 60_{unit} armchair type and two SWCNTs with (5,0) x 30_{unit} zigzag type, respectively. Periodic boundary condition was applied along the axial direction of one of the SWCNT, say Z-axis. Another SWCNT was 90 degree perpendicular to the first one, aligning along Y-axis with the tube ends saturated with hydrogen bonds. Five possible geometries of 3-D (3,3)-(3,3) armchair type X-junctions were constructed, namely A,B,C,D and E as shown in figure 1. All the five types of junctions are energetically stable, with sp^2 hybridized carbon bonds [17]. All the structures are complying with the generalized Euler's rule: the bond surplus at each step must be +12 [19]. Similar five 3-D X junctions are also obtained for (5,0)-(5,0) zigzag.

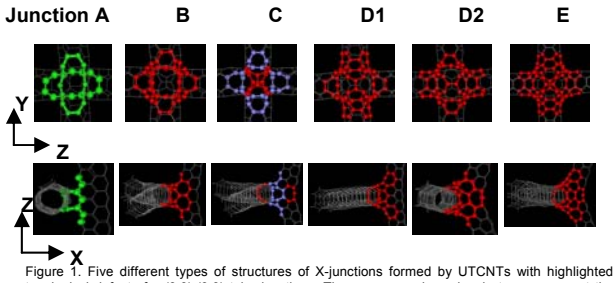

Figure 1. Five different types of structures of X-junctions formed by UTCNTs with highlighted topological defects for (3,3)-(3,3) tube junctions. The green, purple and red atoms represent the atomic structure of enneagons, octagons and heptagons respectively. Junction A includes 4 enneagons; junction B includes 12 heptagons; junction C includes 4 heptagons and 4 octagons; junction D (D1 and D2) includes 12 heptagons; junction E also includes 12 heptagons.

3 SIMULATION RESULTS

In our early study on mechanical properties of junctions under uni-axial tension [17], it was found that different junctions behaved in different ways during the deformation. Similar results were obtained under bi-axial tensile strain. Figure 2a and 2b compare the tensile deformation behavior for those junctions under uni-axial strain along Z-direction and bi-axial strain along both Z and Y-directions for (3.3)-(3,3) and (5,0)-(5,0) X-junctions. We only compare the deformation behavior along Z-axis for the above two cases because (i) junctions A, B, C and E are geometrically symmetric along two directions, the two branches of the junction along Y and Z axes are expected to behave similarly; (ii) for junction D that is not symmetric, we only show the weaker branch of the junction, i.e. the Z-direction in D2 (or Y-direction in D1).

In the case of the armchair (3,3)-(3,3) junctions, it was found that for both uni-axial or bi-axial strain, junctions A, B and D1 exhibited the typical deformation behavior of an SWCNT with all three stages: stage 1 – elastic elongation controlled by altering C-C bond angles; stage 2 – elastic elongation controlled by altering the C-C bond length; and stage 3 – rapid energy release associated with an irreversible bond breaking process [20]. However, junctions C, D2 and E exhibited only two stages, stage 1 and stage 3. Simulation results showed that the deformation behavior at the first stage was the same for all 5 types of X-junctions (strain < 0.18). From figure 4a, one can see that tensile strengths in uni-axial and bi-axial strain cases are similar with small variations for junctions A and B. However, for the junctions C, D2 and E, the tensile strengths are higher in bi-axial strain case than that in uni-axial strain case. The (5,0)-(5,0) zigzag X-junctions seldom show stage 2 during deformation, therefore their tensile properties are similarly to (3,3)-(3,3) junctions C, D2 and E. In general, no matter it is (3,3)-(3,3) junctions or (5,0)-(5,0) junctions, tensile strength of X-junctions decreases with the increase in plastic deformation. One can find some load drops in figure 4b. These load drops indicate that the junctions can withstand the second, third or more elastic loadings after the first plastic deformation associated with bond breaking and reconstruction. This observation is consistent with our early study [17]. The C-C bond reconstructions during deformation have been explained in detail in our early report.

For some of the (3,3)-(3,3) armchair X-junctions (such as junction C), there was clearly a second elastic behavior after the first plastic deformation associated with the bond breaking and reconstruction in figure 2a (blue lines). Therefore, a closer examination of this case was performed.

As shown in figure 3, four independent simulations on junction C were conducted with different random number seeds used to assign the initial momentums for all carbon atoms. It was found that in simulation 1 and 3, the first load drop happened at a strain around 0.2, followed by a significant elastic deformation until the second load drop. However, in simulation 2 and 4, the junction sustained a higher tensile load, followed by a significant load drop. The above results indicate the fact that even for the same junction and nominally same simulation conditions, the outcome of the simulations can be different, depending on the choice of random number seed. This is understandable because the number of carbon atoms involved near the junction region is small. Therefore, the mechanical behavior of the junction will be sensitive to the thermal fluctuation near the junction region.

The upper snapshots in figure 3 show the atomic structures of junctions obtained by simulation 4 in four stages with respect to the tensile force – strain curves on YZ plane and XY plane, respectively. Snapshot M1 shows atomic structure of junction C with highest loading. At that moment, no plastic deformation occurred. From the snapshot M1 on XY plane, one can clearly see the 3-D junction. When plastic deformation started (snapshot M2), bond breaking happened, followed by necking and reconstruction of bonds near the right hand side of the junction on YZ plane. At the same time, the junction area started to move from 3-D like to 2-D type progressively, evident in snapshots on XY plane. As strain continued, the necking was extended and eventually was broken. From the start of plastic deformation to the break down of the junction, an applied strain of less than 0.01 was required (about $2x10^{-15}$ seconds).

The lower snapshots in figure 3 show the junction structures of simulation 1 in five snapshots with respect to the tensile force vs. strain curve. Similarly, the snapshot M1 shows the same junction structure as in simulation 4 before plastic deformation. M2 is the onset of plastic deformation which involved one or two bond reconstruction in the center of the junction. Then, more bond breaking and reconstruction happened in snapshot M3. The major difference between simulation 1 and 4 is that the necking happened on both sides of the junction for simulation 1. This situation resulted in a significant "elastic deformation" after necking. Two necks were extended symmetrically as the applied strain increased, and the load was carried evenly by the two necks. At the moment of M3, the 3-D junction became 2-D like. A second load drop happened until one of the necks broke down (see M5). The breaking process

NSTI-Nanotech 2009, www.nsti.org, ISBN 978-1-4398-1784-1 Vol. 3, 2009

(from M2 to M5) in simulation 1 was relatively slow with an increased applied strain of more than 0.1 (about $10x10^{-15}$ seconds). Similar results were observed in all five (5,0)-(5,0) junctions.

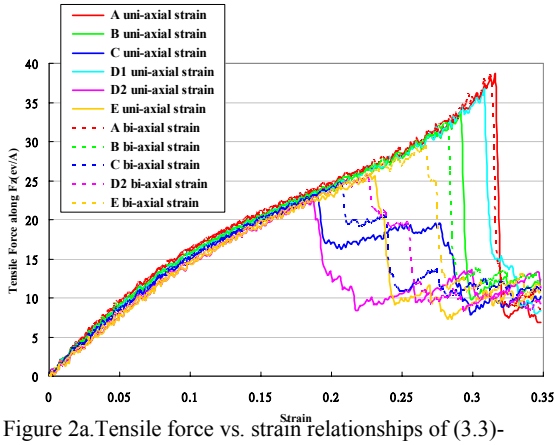

Figure 2a.Tensile force vs. strain relationships of (3.3)-(3,3) 3-D X-junctions under uni-axial and bi-axial tensile strain tests.

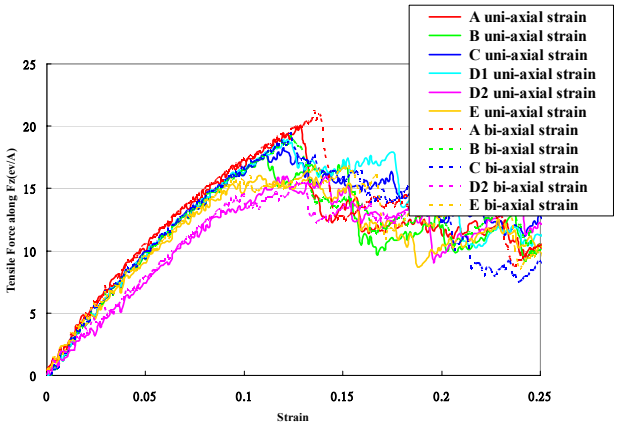

Figure 2b. Tensile force vs. strain relationships of (5,0)-(5,0) 3-D X-junctions under uni-axial and bi-axial strain tests. bi-axial tensile strain tests.

We also conducted 8 simulation trials for junction A and D2 with different random number seeds. However, only one failure mode was observed for junction A with a 5% variation in failure strain. Necking nucleated a distance away from the junction region. This indicates that for junction A, the junction region is stronger than a SWCNT. During the whole necking process, the X-junction remained as a 3-D junction [16]. For junction D2, the results were similar to that of junction C, that is, two different failure modes were observed.

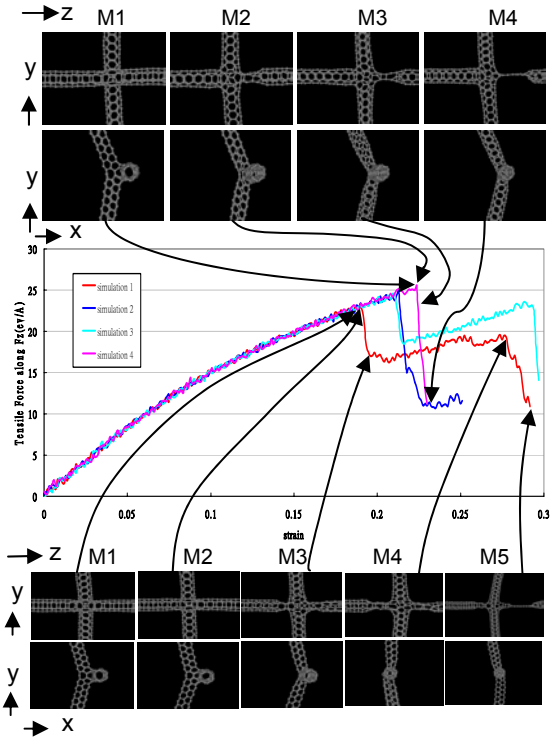

Figure 3. Results of four simulations with different random seed number for (3,3)-(3,3) X-junction C. The upper and lower snapshots show the atomic configurations for necking processing of simulation 4 and 1, respectively.

4 CONCLUSION

Mechanical stability of 3-D ultrathin carbon nanotube X-junctions were studied using systematic molecular dynamics simulations. Five different defect configurations of the (3,3)-(3,3) junctions and (5,0)-(5,0) junctions were studied.

(1) Deformation behavior of X-junctions depends on defect structures at the junction region, with the junction A as the strongest junction;

(2) Some 3-D X-junctions become 2-D X-junctions under tensile strain. Bond breaking and reconstruction at the junction region may result in either one side necking, or necking on both side of the junctions;

(3) Random seed number pays an important role in the outcome of MD simulation. This is due to the small number of carbon atoms involved in the junction region;

(4) The 3-D X-junctions either exhibit the typical behavior of an SWCNT with all three stages of deformation, or show only two stages of deformation when necking occurs near the junctions. For the second case, necking may occurs on one side or on both sides of the junctions. If it occurs in both sides, a significant second elastic deformation process can be observed after the first bond breaking and reconstruction;

(5) For those junctions having typical behavior of an SWNT with all three stages, a single neck far away from the junction region would nucleate and extend until failure.

In this case, the junction region is stronger than the strength of a SWCNT, and the 3-D junction will remain as 3-D;
(6) Failure will be significantly faster if only one side of the junction forms a necking.

Acknowledgments

This work was supported by research grants from the Research Grant Council of Hong Kong (PolyU5265/07E, and HKUST9/CRF/08).

REFERENCES

[1] S. Iijima, Nature 354, 56, 1991.
[2] H. F. Ye, J. B. Wang and H. W. Zhang, Comput. Mater. Sci. doi:10.1010/j.commatsic.2008.07.023.
[3] J. Zou, B. H. Ji, B. Q. Feng and H. Gao, Nano Lett. 6, 430, 2006
[4] M. F. Yu, O. Lourie, M. J. Dyer, K. Moloni, T. E. Kelly and R. S. Ruoff, Science 287, 637, 2000.
[5] S. Iijima, C. Brabec, A. Maiti and J. Bernholc, J. Chem. Phys. 104, 2089, 1996.
[6] T. W. Tombler, C. Zhou, J. Kong, H. Dai, L. Liu, C. S. Jayanthi, M. Tang and S. Y. Wu, Nature 405, 769, 2000.
[7] K.T. Lau and S.Q. Shi, Carbon, Vol. 40, pp.2965~2968, 2002.
[8] K.T. Lau, S.Q. Shi, L.M. Zhou and H.M. Cheng, Journal of Composite Materials, 37 (4): 365-376, 2003.
[9] M. Menon and D. Srivastava, Phys. Rev. Lett. 79, 4453, 1997.
[10] F. Cleri, P. Keblinski, I. Jang and S. B. Sinnott, Phys. Rev. B 69, 121412(R), 2004.
[11] I. Jang, S. B. Sinnott, D. Danailov and P. Keblinski, Nano Lett. 4, 109, 2004.
[12] Y. Yao, Q. Li, J. Zhang, R. Liu, L. Jiao, Y. T. Zhu and Z. LIU, Nature Materials, 6, 283, 2007
[13] M. Ouyaing, J. Huang, C. L. Cheung and C. M. Lieber, Science, 291, 97, 2001.
[14] S. Melchor and J. A. Dobado, J. Chem. Inf. Comput. Sci. 44, 1639, 2004.
[15] Z. Qin, Q. Qin and X. Feng, Physics Letters A, 372, 6661, 2008.
[16] F. Y. Meng, S. Q. Shi, D. S. Xu and R. Yang, Phys. Rev. B, 70, 125418, 2004.
[17] F. Y. Meng, S. Q. Shi, D. S. Xu and C. T. Chan, Modelling Simul. Mater. Sci. Eng., 14, S1-S8, 2006.
[18] D. W. Brenner, O. A. Shenderova, J. A. Harrison, S. J. Stuart, B. Ni and S. B. Sinnott, J. J.Phys.: Condens. Matter, 14, 783, 2002.
[19] V. H. Crespi, Phys. Rev. B, 58, 12617, 1998.
[20] L. G. Zhou and S.Q.Shi, Comput. Mater. Sci. 23, 166, 2002.